FULL PAPER

Bioinspired Blood Compatible Surface Having Combined Fibrinolytic and Vascular Endothelium-Like Properties via a Sequential Coimmobilization Strategy

Wenjun Zhan, Xiujuan Shi, Qian Yu, Zhonglin Lyu, Limin Cao, Hui Du, Qi Liu, Xin Wang, Gaojian Chen, Dan Li, John L. Brash, and Hong Chen**

Developing surfaces with antithrombotic properties is of great interest for the applications of blood-contacting biomaterials and medical devices. It is promising to coimmobilize two or more biomolecules with different and complementary functions to improve blood compatibility. However, the general one-pot strategy usually adopted by previous studies suffers the problems of inevitable competition between diverse biomolecules and uncontrollability of the relative quantities of the immobilized biomolecules. To solve these problems, a new sequential coimmobilization strategy is proposed and applied to fabricate a blood compatible surface. Polyurethane surface is modified with a copolymer, poly(2-hydroxyethyl methacrylate-co-1-adamantan-1-ylmethyl methacrylate), which serves as a linker-spacer for sequential attachment of two functional molecules, a hexapeptide containing REDV (Arg-Glu-Asp-Val) sequence, and a modified cyclodextrin bearing 7 lysine ligands, through covalent bonding and host–guest interaction, respectively. The resulting surface combines the antithrombogenic properties of the vascular endothelium and the clot lysing properties of the fibrinolytic system. Importantly, neither of the two functions of REDV peptide and lysine is compromised by the presence of the other, suggesting the enhanced blood compatibility. These results suggest a new strategy to engineer multifunctional surfaces by coimmobilization of bioactive molecules having unique functionalities.

1. Introduction

Coagulation and thrombosis on the surfaces of synthetic materials in direct contact with blood cause a variety of serious problems including failure of artificial organs, implants in the cardiovascular system, and extracorporeal blood-contacting medical devices.[1] Therefore, it is of great interest to endow surfaces with antithrombogenic properties.[2] Much work has been reported based on a defensive strategy from the fibrinogenesis point of view.[3] In this strategy, surfaces are either modified with hydrophilic nonfouling polymers (e.g., polyethylene glycol (PEG)) to suppress plasma protein adsorption and platelet adhesion,[4] and/or with bioactive molecules such as the anticoagulant heparin to prevent the formation of thrombus.[5] To date, however, this approach has not produced any material that is sufficiently resistant to thrombus formation. Alternatively, we and other groups have proposed an offensive strategy whereby the fibrinolytic system is activated so that nascent clots that form on the surface are broken down.[6] Based on this strategy, we have developed several surfaces which were shown to capture plasminogen (Plg) and tissue type plasminogen activator (t-PA) selectively when in contact with blood to generate plasmin and lyse nascent clots formed on the surface.[7]

Although effective with respect to clot lysis, these surfaces are not actively antithrombogenic. The vascular endothelium (the inner surface of blood vessels) is the gold standard in this regard and is the only known surface that is blood compatible in all respects.[8] Accordingly surface endothelialization has been widely practiced as a strategy for the realization of blood compatible materials.[9] Immobilization of antibodies against cell surface antigens[10] or cell adhesive peptides[11] has been shown to promote the adhesion and proliferation of endothelial cells (ECs) on material surfaces. However, it has also been shown that when the growth of endothelial cells is promoted by immobilized bioactive molecules, the anticoagulant properties deteriorate.[12] In the present paper we describe a

W. Zhan, X. Shi, Prof. Q. Yu, Z. Lyu, Dr. L. Cao, H. Du, Q. Liu, X. Wang, Prof. G. Chen, Prof. D. Li, Prof. J. L. Brash, Prof. H. Chen
College of Chemistry
Chemical Engineering and Materials Science
Soochow University
Suzhou, Jiangsu 215123, P. R. China
E-mail: yuqian@suda.edu.cn; chenh@suda.edu.cn
Prof. G. Chen
Center for Soft Condensed Matter Physics and Interdisciplinary Research
Soochow University
Suzhou, Jiangsu 215006, P. R. China
Prof. J. L. Brash
School of Biomedical Engineering and Department of Chemical Engineering
McMaster University
Hamilton, Ontario L8S4L7, Canada

DOI: 10.1002/adfm.201501642

method for the coimmobilization of biomolecules having different and complementary functionalities such that interactions between the two molecules leading to loss of functionality are avoided. The method is applied to the preparation of surfaces that are able both to lyse nascent clots and promote endothelialization.

Many methods have been developed for the immobilization of biomolecules on surfaces including physical adsorption, covalent bonding, ionic bonding, and bioaffinity immobilization.[13] Coimmobilization of diverse biomolecules, however, remains a challenging task. In general a one-pot process is used in which the substrate is immersed in a solution containing both biomolecules.[14] Competition between the biomolecules is, however, inevitable, making it difficult to control the relative quantities of the biomolecules bound to the substrate. One possible approach to solve these problems is immobilization of different biomolecules through respective independent methods step by step. Host–guest interaction is a versatile and robust noncovalent binding method to incorporate biomolecules onto surfaces. This method is milder, and therefore less likely to compromise the activity of the ligands, than methods that relied on covalent immobilization.[15] The mechanisms of host–guest interaction and covalent bonding are different, it is thus expected that the combination of these two methods for sequential coimmobilization of diverse biomolecules will avoid competition for the surface and facilitate control of the relative quantities of immobilized biomolecules. To our best known, however, few studies were reported on this aspect.

Herein, we report on using a new sequential coimmobilization strategy to fabricate bioinspired blood compatible surface having combined vascular endothelium-like and fibrinolytic properties. Specifically, two ligands, a peptide with the Arg-Glu-Asp-Val (REDV) sequence and a β-cyclodextrin derivative bearing seven lysine ligands (β-CD-$(Lys)_7$) were incorporated into polyurethane (PU) surfaces. REDV peptide is a fibronectin-derived peptide and has been widely used as a ligand for ECs that selectively promotes the adhesion, spreading and proliferation of ECs in preference to smooth muscle cells and platelets; previous studies have demonstrated that REDV sequence is one of the main recognition sites for integrin $\alpha4\beta1$binding, which leads to specific interaction between fibronectin and ECs.[11] Lysine is a ligand with high affinity for Plg and t-PA, facilitating the generation of plasmin to lyse incipient clots.[6a] To incorporate these two ligands, PU surfaces were modified with a copolymer of poly(2-hydroxyethyl methacrylate-*co*-1-adamantan-1-ylmethyl methacrylate) (poly(HEMA-co-AdaMA)), which provides attachment sites for REDV peptide through covalent bonding, and for β-CD-$(Lys)_7$ through host–guest interaction. The successful preparation of this surface was confirmed using a series of characterization methods and assays. Protein adsorption, plasma clot lysis, and cell culture experiments demonstrated that the dual-modified surfaces maintained the functionalities of the lysine and the REDV peptide. Moreover, neither of the two functions was compromised by the presence of the other.

2. Results and Discussion

2.1. Synthesis of β-CD-$(Lys)_7$

In this work, we adopted host–guest interactions, a versatile and robust noncovalent binding method to incorporate lysine into the PU surface. β-cyclodextrin (β-CD) and adamantane (Ada) are a strongly interacting pair and have been widely used as linkers for the integration of biomolecules to construct functionalized biosubstrates.[16] In addition, β-CD is an appropriate template with multivalent binding sites for postmodification to increase the local density of ligands.[17] Our previous work demonstrated that increase of local density of lysines on lysine-substituted β-CD resulted in higher Plg adsorption and higher Plg binding affinity.[18] Therefore, we chose to fully substitute 7 primary hydroxyl groups located on the narrower ring of β-CD with lysine ligands to enhance the binding of Plg and leave the wider ring of β-CD remaining open for further β-CD-Ada binding. The synthesis of a β-CD-$(Lys)_7$ complex is illustrated in **Scheme 1** and the composition of the product was determined by nuclear magnetic resonance spectroscopy (NMR) and Fourier transform infrared spectroscopy (FTIR, see Supporting information, Figure S4). As shown in **Figure 1**, characteristic peaks at 3.16–3.80 and 7.75 ppm, attributed to the protons of CD residues and NH_2, respectively, indicate the successful incorporation of lysine into the CD ring. The calculation results based on NMR peak area demonstrated that each β-CD-$(Lys)_7$ contains seven lysine ligands.

2.2. Preparation and Characterization of PU-REDV/Lys Surfaces

The preparation of PU-REDV/Lys surfaces involved several steps as illustrated in **Scheme 2**. First, methacryloylisothiocyanate (MI) was coupled to PU surface to introduce vinyl groups, followed by grafting of a copolymer of HEMA and AdaMA (PHA) via surface-initiated radical polymerization.[19] The molecular weight (MW) of the grafted PHA on the PU surface was about 7.7×10^4 as determined by measuring the MW of free polymer formed simultaneously in solution,[20] and the grafting density of PHA was about 4.0 mg cm^{-2} as measured by gravimetry.[21] The PHA copolymer containing two pendant functional groups (OH from HEMA and Ada from AdaMA) then served as a spacer-linker for incorporation of the REDV and Lys ligands to obtain hybrid surfaces referred to as PU-REDV/Lys. The OH groups were activated by 4-nitrophenyl chloroformate (NPC) to covalently couple REDV peptide via the formation of amide bonds, while Ada groups were

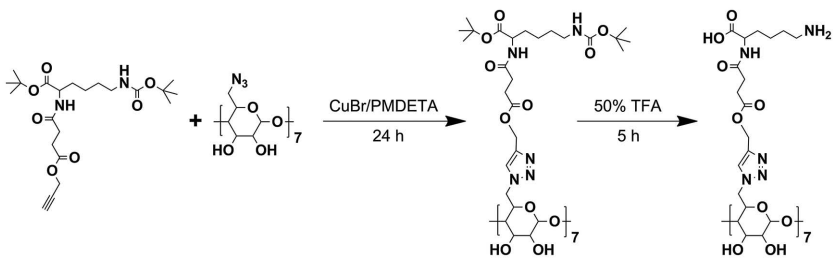

Scheme 1. Synthetic route of β-CD-$(Lys)_7$.

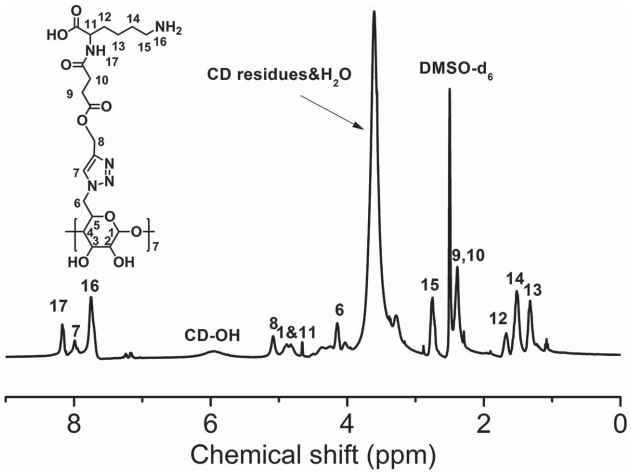

Figure 1. ^{1}H NMR spectrum of β-CD-(Lys)$_7$.

used to incorporate β-CD-(Lys)$_7$ via host–guest interaction. As mentioned above, coimmobilization of different biomolecules is usually performed by immersing the material in a solution containing both biomolecules, with the risk of competition for the surface; also the relative amounts of the immobilized biomolecules cannot be controlled. However, because in our system the molecules are introduced sequentially and immobilized using different methods, competing reactions are avoided and the relative content of two molecules can be easily adjusted by changing the ratio of poly(HEMA)/poly(AdaMA) during the polymerization. As controls, surfaces modified with only REDV peptide or β-CD-(Lys)$_7$ were also prepared; these are referred to as PU-REDV and PU-Lys, respectively.

Changes in chemical composition and surface wettability of the PU surfaces after each modification step were monitored by X-ray photoelectron spectroscopy (XPS) analysis and contact angle goniometry, respectively (**Table 1**). The appearance of sulfur on the PU-PHA surfaces indicated the attachment of MI, and the decrease of water contact angle (from 75.8° ± 0.7° to 61.6° ± 0.8°) confirmed that grafting of PHA, with its hydrophilic poly(HEMA) component, was successful. The immobilization of REDV peptide and β-CD-(Lys)$_7$ on the PU-PHA surface was qualitatively confirmed by the increase in nitrogen seen in the low resolution XPS. The amounts of surface-immobilized REDV peptide and lysine were quantitatively determined by p-nitrophenol assay and acid orange II assay as 0.082 ± 0.006 and 0.95 ± 0.01 nmol cm^{-2}, respectively (see the Supporting Information for details).

2.3. Protein Adsorption

We first measured protein adsorption from plasma to the modified surfaces because it is well accepted that protein adsorption is the initial event when a material comes into contact with blood and that the adsorbed protein layer influences subsequent interactions such as clotting.[22] Fibrinogen (Fg) was used as a model protein since it is abundant in plasma, and since adsorbed Fg is known to be a key component of the protein layer on many materials and to be a key ligand for platelet adhesion.[23] As shown in **Figure 2**, fibrinogen adsorption on the PU-PHA surface was reduced by ≈85% compared to the unmodified PU, presumably due to the protein resistance of the poly(HEMA) component. Subsequent introduction of REDV peptide and β-CD-(Lys)$_7$ into the PU-PHA surface resulted in a slight increase in Fg adsorption but the absolute level remained low (<30 ng cm^{-2}). The slight loss of protein resistance was presumably due to the decreased concentration of hydroxyl groups on the surface and to electrostatic interactions between the partially protonated amino groups and the negatively charged Fg. In addition, adsorption of another important protein, human serum albumin (HSA) from plamsa to sample surfaces was evaluated (Supporting information, Figure S6). Similar to the result of Fg adsorption, it is found that compared with unmodified PU surface, PU-REDV/Lys surface reduced more than 82% of HSA adsorption, indicating good resistance against nonspecific protein adsorption.

We then investigated the adsorption of Plg, the central protein of the fibrinolytic system.[6a] Both Plg and t-PA are known to bind to lysine moieties on the surface of fibrin clot via their lysine binding sites to form a ternary complex whereby Plg is activated to plasmin; therefore, lysine has been used as a ligand for binding Plg.[24] As shown in Figure 2, the surfaces without

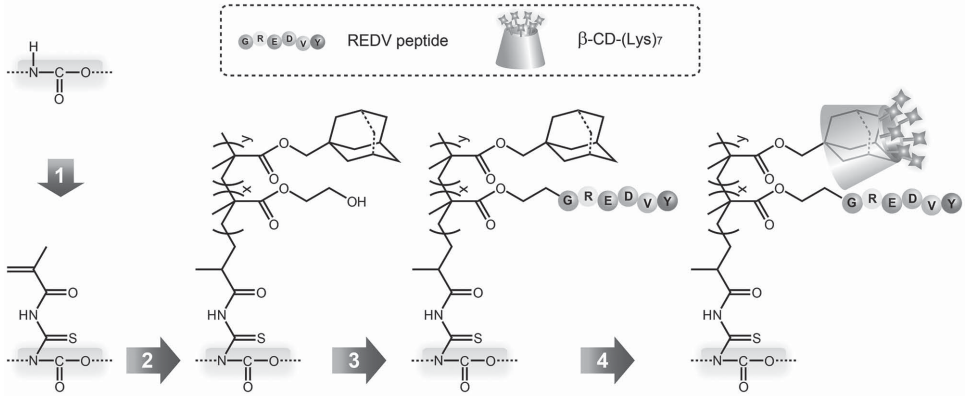

Scheme 2. Schematic depicting the procedure for preparation of PU-REDV/Lys surfaces. Step1: preparation of vinyl-functionalized PU (VPU) surfaces; Step 2: polymerization of HEMA and AdaMA from VPU; Step 3: Conjugation of REDV peptide to PHA via covalent bonding; Step 4: Immobilization of β-CD-(Lys)$_7$ onto PHA via host–guest interactions.

Table 1. Elemental composition and water contact angle of PU surfaces after each modification step.

Surface	Elemental composition [%]				Water contact angle[a)] [°]
	C	N	O	S	
PU	72.0	3.1	24.9	N.D.	75.8 ± 0.7
PU-PHA	70.7	2.8	26.3	0.2	61.6 ± 0.8
PU-REDV	68.8	4.6	26.6	0.1	64.8 ± 1.0
PU-REDV/Lys	70.2	4.5	25.2	0.1	54.3 ± 0.8

[a)]Contact angle data are mean ± standard error ($n = 6$).

lysine exhibited low levels of Plg adsorption (<20 ng cm^{-2}), suggesting that nonspecific adsorption of this protein is limited. In contrast, the introduction of lysine increased the adsorption of Plg to both PU-Lys and PU-REDV/Lys surfaces to levels >1.55 μg cm^{-2}), i.e., a greater than tenfold increase compared to the unmodified PU. It is important to note that the adsorbed quantities of Plg on the PU-Lys and PU-REDV/Lys surfaces are not different ($p > 0.05$), suggesting that the REDV peptide did not affect the binding of Plg to lysine. In summary, these data show that the PU-REDV/Lys surfaces suppressed nonspecific protein adsorption and promoted the specific adsorption of Plg, both effects being favorable for blood compatibility.

2.4. Plasma Clot Lysis

We investigated the fibrinolytic function of the modified surfaces using a plasma clot lysis assay as reported previously.[7c] The detailed procedure can be found in the Experimental Section: briefly the surfaces were immersed in plasma allowing the lysine residues to adsorb a layer of plasminogen; they were then exposed to t-PA to convert plasminogen to plasmin; finally they were immersed in recalcified citrated plasma and coagulation was observed by measuring the absorbance of the plasma at 405 nm over time. Typical data are shown in **Figure 3**. The onset of coagulation is indicated by a steep

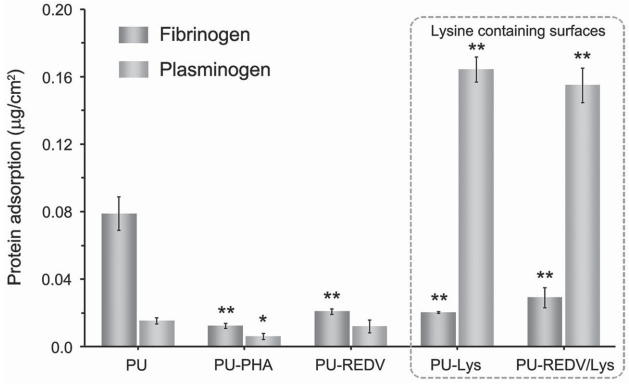

Figure 2. Adsorption of fibrinogen and plasminogen from plasma (3 h exposure) on unmodified and modified PU surfaces. Error bars represent the standard deviation of the mean ($n = 3$). Comparison of data between unmodified and modified PU surfaces were analyzed using a one-way ANOVA (* $p < 0.05$; ** $p < 0.01$).

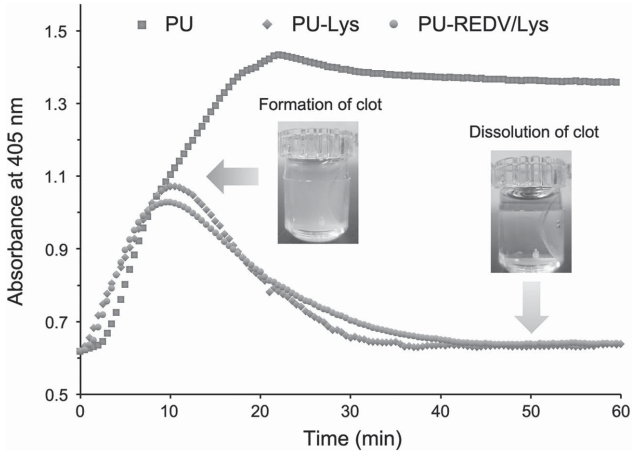

Figure 3. Clot formation in plasma expressed as absorbance at 405 nm versus time for unmodified and modified PU surfaces. The insets show the visual appearance of the plasma at different times.

rise in the absorbance versus time curve. The unmodified PU surface showed a typical clot formation response: the absorbance reached a plateau value which was maintained over time. In contrast, for the lysine-containing surfaces, the absorbance rose during the first 10 min, and then fell, eventually returning to baseline after 40 min. These observations suggest that although clot formation was initiated, the incipient clot was soon lysed by the action of surface localized plasmin as generated from the adsorbed Plg after activation by t-PA. Again, it was found that the PU-REDV/Lys surface exhibited almost the same fibrinolytic activity as the PU-Lys surface, demonstrating that the immobilized REDV peptide did not affect the activity of the lysine. Besides the fibrinolytic function, we also investigated the in vitro hemocompatibility of the modified surfaces by testing the platelet adhesion, plasma recalcification time (PRT), and hemolysis of the blood. The results indicated that the PU-REDV/Lys surface not only could lyse incipient clots but also exhibited improved hemocompatibility compared with unmodified PU surface (see the Supporting Information for details).

2.5. Adhesion and Proliferation of Endothelial Cells

Finally, we investigated the adhesion and proliferation of endothelial cells on the modified surfaces (see the Experimental Section for details). As shown in **Figure 4**, after 4 h of culture, the number of adherent cells on the PU-PHA surface was significantly lower than on the PU ($p < 0.05$), possibly due to the protein- and cell-repellent properties of the poly(HEMA) component. However, the introduction of REDV peptide resulted in a dramatic increase in cell attachment, with the adherent cell density about threefold greater than on the PU surface. This remarkable enhancement in cell attachment shows the strong affinity between ECs and surface immobilized REDV peptide. The morphology of the adherent cells was observed using fluorescence microscopy; for this purpose the cells were stained with DAPI (blue fluorescence, for nuclei) and phalloidin-FITC (green fluorescence, for actin fibers). As

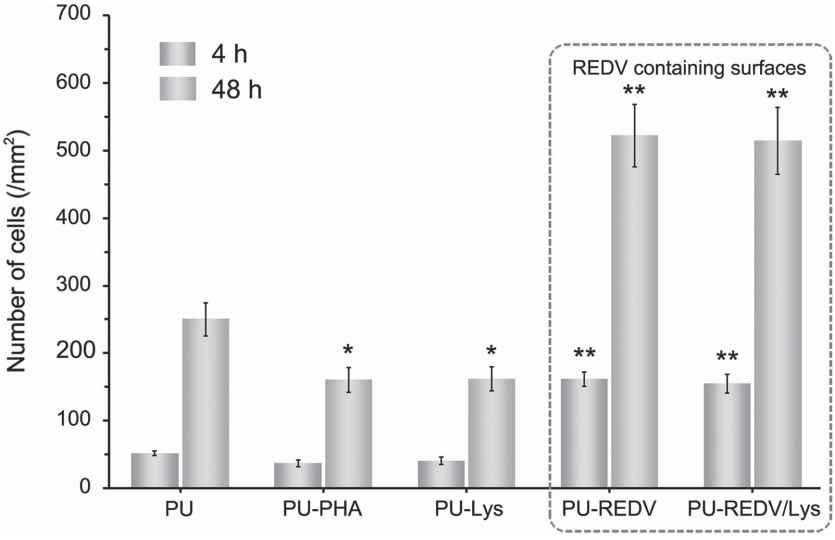

Figure 4. Density of adherent endothelial cells on unmodified and modified surfaces after culture for 4 and 48 h. Error bars represent the standard deviation of the mean ($n = 3$). Comparison of data between unmodified and modified PU surfaces were analyzed using a one-way ANOVA (* $p < 0.05$; ** $p < 0.01$).

shown in **Figure 5** (upper panels), on peptide-containing surfaces, the endothelial cells showed normal morphology, indicating good cytocompatibility of the surface. Furthermore, the proliferation of ECs on the surfaces was studied after 48 h culture. Again, there were obviously more cells on the peptide-containing surfaces compared with the unmodified PU, and the attached cells on these surfaces were well spread to form a confluent layer (Figure 5, lower panels). The normal function of adherent ECs was demonstrated by testing accumulative NO release by ECs on the modified surfaces (Supporting information, Figure S9). It is beneficial for the applications of blood vessel materials that the surfaces can promote the adhesion and proliferation of ECs as well as suppress the adhesion and growth of smooth muscle cells (SMCs). We found that for PU-REDV/Lys surface, the introduction of REDV peptide resulted in a slight increase in cell attachment compared with PU-PHA surface, but still significantly lower than on the PU surface ($p < 0.01$, Supporting information, Figure S10), suggesting that the presence of REDV peptide is selectively favorable for adhesion, spreading and proliferation of ECs.[11] These data together indicate that in situ endothelialization of the PU-REDV/Lys surface is possible and suggest that the resulting surface will show endothelium-like long-term blood compatibility. Again it should be noted that the densities of adherent cells on the PU-REDV and PU-REDV/Lys surfaces are not different and the cellular morphology is essentially the same on both, indicating that the presence of lysine did not compromise the interactions of the REDV with ECs. Together with the protein adsorption and plasma clot lysis assay, it is concluded that the PU-REDV/Lys surface maintained both the specific functionality of lysine (for selective adsorption of Plg and clot lysis) and REDV peptide (for promotion of adhesion and proliferation of ECs). Moreover, neither of the two functions was compromised by the presence of the other, suggesting the enhanced blood compatibility.

3. Conclusion

In summary, we have developed a novel multifunctional surface for blood contacting applications with the ability to lyse incipient clots generated in the early stages of contact and to promote endothelialization for longer-term hemocompatibility. These specific functionalities were realized by the sequential incorporation of two ligands, β-CD-$(Lys)_7$ and REDV peptide, into the surfaces by host–guest interaction and covalent bonding, respectively. The resulting PU-REDV/Lys surface was shown to resist nonspecific protein adsorption from plasma but to promote selective adsorption of plasminogen, thereby facilitating fibrinolytic activity. At the same time, this surface promoted the adhesion and proliferation of endothelial cells. Moreover, neither of the two functions was compromised by the presence of the other. This system, for the first time, demonstrates two different strategies (host–guest interaction and covalent bonding) for the sequential immobilization of two biomolecules with their respective bioactivities such that competition for the surface is avoided and control of the relative quantities of immobilized biomolecules is facilitated. Clearly, this approach constitutes a design platform, not limited to the lysine and REDV peptide pair, but applicable to other combinations of bioactive molecules having unique functionalities. Considering these generality and versatility attributes, this work may provide a new methodology for the

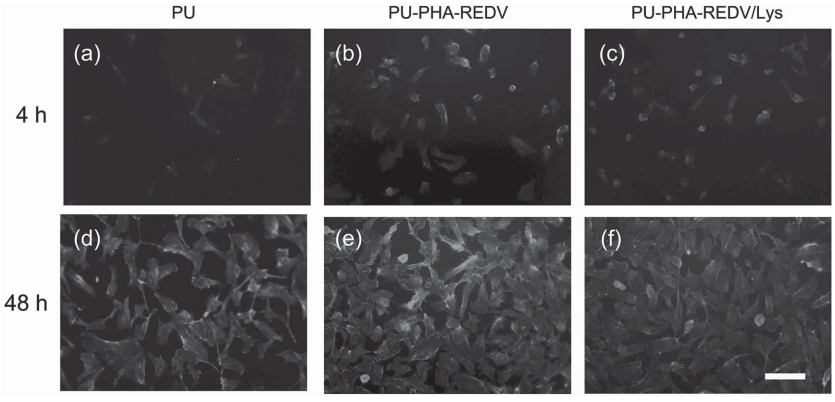

Figure 5. Dual channel (blue/green) fluorescence images of endothelial cells on unmodified and modified PU surfaces after culture for 4 and 48 h. The cells were fixed and stained with DAPI for nuclei (blue) and Phalloidin-FITC for actin (green), respectively. Scale bars represent 100 μm.

engineering of multifunctional surfaces for a variety of practical applications in the biomedical and biotechnology fields.

4. Experimental Section

Materials: Tecothane polyurethane (PU, TT-1095A, Thermedics) was purified by Soxhlet extraction with methanol and toluene for 72 h to remove impurities and dried in a vacuum oven at 50 °C for 48 h. Per-6-azido-β-cyclodextrin (β-CD-$(N_3)_7$),[25] methacryloyl isothiocyanate (MI),[19] and 4-Oxo-4-(prop-2-yn-1-yloxy) butanoic anhydride[26] were synthesized as reported previously. The adamantane monomer, 1-adamantan-1-ylmethyl methacrylate (AdaMA) was synthesized as described in the Supporting Information. Copper (I) bromide (CuBr, 98%, Sigma-Aldrich) was washed successively with acetic acid and ethanol and dried in a vacuum oven prior to use. 2,2′-Azoisobutyronitrile (AIBN) from Sinopharm Chemical Reagent Co. (Shanghai, China) was recrystallized from ethanol solution and dried under vacuum. 2-hydroxyethyl methacrylate (HEMA) (98%, Acros) was purified by passing over an "inhibitor removal column."[7d] "Inhibitor removers," trifluoroacetic acid (TFA), *N*,*N*,*N*′,*N*″, *N*″-pentamethyldiethylenetriamine (PMDETA, 99%) and 4-nitrophenyl chloroformate (NPC, 96%) were obtained from Sigma-Aldrich Chem. Co. and used as received. All organic solvents were purchased from Sinopharm Chemical Reagent Co. (Shanghai, China) and purified according to standard methods before use. Gly-Arg-Glu-Asp-Val-Tyr (GREDVY) peptide was purchased from GL Biochem Ltd. (Shanghai). Fibrinogen was purchased from Calbiochem (LaJolla, CA). Plasminogen was purchased from Enzyme Research Laboratories (South Bend, IN). Tissue plasminogen activator (t-PA) was purchased from Genentech (San Francisco, CA). $Na^{125}I$ was obtained from Chengdu Gaotong Isotope Co., Ltd (China). Endothelial cell medium (ECM) with growth supplement was from ScienCell Research Laboratories (Carlsbad, CA). Human umbilical vein endothelial cells (HUVECs) were provided by the Second Affiliated Hospital of the Medical College of Zhejiang University.

Surface Preparation: Synthesis of β-Cyclodextrin Derivative with Seven Lysine Ligands (β-CD-$(Lys)_7$): The preparation process for 6-tert-butoxycarbonyl amino-2-(4-oxo-4-(prop-2-yn-1-yloxy)butanamido)-hexanoic acid tert-butyl ester (Lys(P)-alkyne) is described in the Supporting Information. β-CD-$(Lys(P))_7$ was synthesized via Cu(I)-catalyzed azide-alkyne cyclization (CuAAC) method. Briefly, Lys(P)-alkyne (704.8 mg, 1.6 mmol) and β-CD-$(N_3)_7$ (262.0 mg, 0.2 mmol) were dissolved in 5 mL dimethyl sulfoxide in a Schlenk tube, then PMDETA (20.9 µL, 0.1 mmol) and CuBr (14.5 mg, 0.1 mmol) were added to the solution. The solution was deoxygenated by three freeze-pump-thaw cycles and stirred at 50 °C for 24 h. Then the reaction mixture was passed through a short alumina column to remove the copper salt and precipitated into cool deionized water. The product was isolated as a yellow solid after freeze drying with a yield of ≈73.3%. ^{1}H NMR (400 MHz, DMSO-d_6, δ): 8.20–8.07 (m, 7H, CO—NH—CH), 7.96 (d, *J* = 20.4 Hz, 7H; NCH═C), 6.76 (t, *J* = 12.8 Hz, 7H; CH_2—NH—CO) 6.00 (d, *J* = 46.5 Hz, 14H; O—2H, O—3H of β-CD), 5.09 (d, *J* = 41.9 Hz, 14H; C—CH_2—O), 4.99–4.70 (m, 14H, C-1H of β-CD, NH—*CH*—CH_2), 4.04 (s, 14H, C—6H of β-CD), 3.80–3.21 (m, overlaps with H_2O, C—2H, C—3H, C—4H, C—5H of β-CD), 2.85(t, *J* = 20.6 Hz, 14H; CH_2—CH_2—NH) 2.60-2.25 (m, overlaps with DMSO-d_6, CO—CH_2—CH_2, CH_2—CH_2—CO), 1.8–1.14 (m, 168H, NHCH—CH_2—CH_2, CH_2—CH_2—CH_2, CH_2—CH_2—CH_2NH, C—CH_3).

^{13}C NMR (400 MHz, DMSO-d_6, δ): 172.46 (CH_2—CO—NH), 171.76 (CH_2—O—CO—CH_2), 171.15 (CH—CO—O—C), 155.99 (NH—CO—O—C), 142.27 (N—CH═C—CH_2), 127.02 (N—CH═C—CH_2), 102.11 (C_{-1} of β-CD), 83.01 (C_{-4} of β-CD), 80.74 (CH—CO—O—C—$(CH_3)_3$), 77.75 (NH—CO—O—C—$(CH_3)_3$), 72.75 (C_{-3} of β-CD), 72.19 (C_{-2} of β-CD), 69.95 (C_{-5} of β-CD), 57.37 (C_{-6} of β-CD), 53.06 (CH═C—CH_2—O), 52.06 (NH—CH—CO), 39.05 (CH_2—CH_2—NH—CO), 31.28 (CO—CH_2—CH_2), 29.81 (CH—CH_2—CH_2), 29.50 (CH—CH_2—CH_2—CH_2—CH_2), 29.04 (CO—CH_2—CH_2—CO), 28.02 (C— $(CH_3)_3$), 27.02 (C—$(CH_3)_3$), 22.89 (CH—CH_2—CH_2—CH_2).

The protective groups in the Lys(P) were removed to obtain β-CD-$(Lys)_7$ by treatment with TFA. 500 mg of β-CD-$(Lys(P))_7$ was dissolved in 6 mL dichloromethane and cooled in an ice bath, then 3 mL TFA was added dropwise to the solution. The mixture was stirred at 0 °C for 1 h and left at room temperature for 4 h. After the solvent was removed by rotary evaporation, the crude product was precipitated into cool diethyl ester. The final product was collected by centrifugation at 10 000 rpm and obtained as a light green solid after vacuum-drying for 24 h with a yield of ≈88.1%. ^{1}H NMR (400 MHz, DMSO-d_6, δ): 8.15 (d, *J* = 21.1 Hz, 7 H; CO—NH—CH), 7.97 (d, *J* = 16.6 Hz, 7 H, NCH=C), 7.68 (s, 14 H, CH_2—NH_2), 6.30—5.50 (m, O_{-2}H, O_{-3}H of β-CD), 5.08 (s, 14 H, C—CH_2—O), 4.98–4.68 (m, 14H, C_{-1}H of β-CD, NH—CH—CH_2), 4.15 (s, 14 H, C_{-6}H of β-CD), 3.90–3.15 (m, overlaps with HOD, C_{-2}H, C_{-3}H, C_{-4}H, C_{-5}H of β-CD). 2.98—2.65 (m, 14H, CH_2—CH_2—NH), 2.60–2.25 (m, overlaps with DMSO-d_6, CO—CH_2—CH_2, CH_2—CH_2—CO), 1.8–0.9 (m, 42H, NHCH—CH_2—CH_2, CH_2—CH_2—CH_2, CH_2—CH_2—CH_2NH).^{13}C NMR (400 MHz, DMSO-d_6, δ): 174.71 (—COOH), 172.06 (CH_2—CO—NH), 170.46 (CH_2—O—CO—CH_2), 141.47 (N—CH═C—CH_2), 126.15 (N—CH═C—CH_2), 101.72 (C_{-1} of β-CD), 82.76 (C_{-4} of β-CD), 72.32 (C_{-3} of β-CD), 71.75 (C_{-2} of β-CD), 69.64 (C_{-5} of β-CD), 56.88 (C_{-6} of β-CD), 54.66 (CH═C—CH_2—O), 52.59 (NH—CH—CO), 39.05 (CH_2—CH_2—NH_2), 31.02 (CO—CH_2—CH_2), 29.62 (CH—CH_2—CH_2), 28.76 (CH—CH_2—CH_2—CH_2—CH_2), 26.60 (CO—CH_2—CH_2—CO), 22.28 (CH—CH_2—CH_2—CH_2).

Preparation of PU-PHA Surfaces: PU films were cast from a 5% (w/v) solution in dimethylformamide and dried at 65 °C for 48 h. The films were then cut into discs, about 0.60 cm in diameter and 0.5 mm in thickness. Vinyl-functionalized PU surfaces (VPU) were prepared as described previously.[19] Poly(HEMA-co-AdaMA)-grafted PU surfaces (PU-PHA) were prepared using surface-initiated free radical polymerization of HEMA and AdaMA from the VPU surfaces. In brief, HEMA (1.15 g, 8.88 mmol), AdaMA (0.026 g, 0.11 mmol) and AIBN (14.8 mg, 0.09 mmol) were dissolved in 8 mL isopropanol. Then VPU films were immersed in the isopropanol solution. After degassing by bubbling with nitrogen for 20 min, the reaction mixture was transferred to an oil bath and stirred at 60 °C for 6 h under a nitrogen atmosphere. When the polymerization was complete, the PU-PHA films were rinsed successively with isopropanol, distilled water, and isopropanol and then dried in a vacuum oven overnight at 40 °C. Meanwhile, the polymerization mixture was diluted with methanol and precipitated in 400 mL diethyl ether. The copolymers formed in solution were collected by centrifugation and dried in a vacuum oven for 24 h.

Preparation of PU-REDV/Lys Surfaces: For the covalent immobilization of REDV peptide on the PU-PHA surface, the hydroxyl groups of the poly(HEMA) component of PHA copolymer were activated by NPC. In brief, the PU-PHA surfaces were incubated in 25 mL anhydrous acetonitrile solution containing 0.51 g of NPC and 0.36 mL triethylamine; then the mixture was stirred at room temperature for 20 h. The NPC-activated PU surfaces (PU-PHA-NPC) were washed thoroughly with acetonitrile, deionized water, and acetone and dried in a vacuum oven at room temperature for 24 h. The PU-PHA-NPC surfaces were then immersed in a REDV peptide solution (0.5 mg mL^{-1} in phosphate buffered saline (PBS), pH 8.2) for 24 h. The surfaces were then treated with 0.5 M ethanolamine to remove any unreacted NPC, washed with PBS (pH 7.4) and deionized water and then dried in a vacuum oven at room temperature for 24 h. The resulting surfaces are referred to as PU-REDV. To incorporate β-CD-$(Lys)_7$, the PU-REDV surfaces were immersed in a 0.5×10^{-3} M β-CD-$(Lys)_7$ aqueous solution for 12 h. The surfaces were rinsed with deionized water and dried in a vacuum oven at room temperature for 24 h. The resulting surfaces are referred to as PU-REDV/Lys. As controls, surfaces incorporating only REDV peptide or β-CD-$(Lys)_7$ were also prepared using the same method as described above. These are referred to as PU-REDV and PU-REDV/Lys, respectively.

Characterization: All prepared compounds were analyzed by nuclear magnetic resonance spectroscopy (NMR) (Varian Inova 400 MHz instrument), with deuterated chloroform or deuterated dimethyl

sulfoxide as solvents. The precipitated polymers were analyzed by gel permeation chromatography (GPC) using a Waters 1515 gel permeation chromatograph with polystyrene standards. DMF was used as the eluent at a flow rate of 0.8 mL min^{-1} operated at 30 °C. Fourier transform infrared (FT-IR) spectra were recorded using the KBr tablet method with a Nicolet 6700 FTIR spectrometer. Typically, 64 scans were collected for each sample. Chemical compositions of the unmodified and modified PU surfaces were determined using an ESCALAB 250 XI X-ray photoelectron spectrometer (Thermo Scientific, USA). The water contact angles of the unmodified and modified PU surfaces were measured with an SL200C optical contact angle meter (Solon Information Technology Co., Ltd.) using the sessile drop method at room temperature. Six replicates were measured for each surface.

Protein Adsorption: Fg and Plg were radiolabeled with $Na^{125}I$ according to our previous work.[7c] To measure protein adsorption from plasma, the radiolabeled proteins were mixed with citrate-anticoagulated pooled normal human plasma (PNP) at an approximate concentration of 10% of the corresponding endogenous protein level. The samples were incubated in PBS for 12 h prior to the adsorption experiments, and then immersed in plasma containing radiolabeled protein (Fg or Plg) for 3 h at room temperature. The samples were removed from the wells, rinsed with PBS three times (10 min each time), wicked onto filter paper and transferred to clean tubes. A Wallac 2480 Wizard 300 automatic gamma counter (Perkin Elmer Life Sciences) was used for radioactivity determination. Adsorption of Fg or Plg was expressed as mass per unit surface area.

Plasma Clot Lysis: The surfaces were immersed in 250 µL of PNP for 3 h at room temperature in 96-well microtitre plate wells, then washed with PBS three times (10 min each time), and transferred to clean wells. 250 µL of t-PA (0.1 mg mL^{-1} in PBS) was added and the wells incubated for 0.5 h at room temperature. The unbound proteins were removed by washing with PBS. This procedure provides surfaces bearing a layer of bound plasmin. To evaluate the fibrinolytic activity of the plasmin-adsorbed sample surfaces, a modified plasma recalcification assay was used. Briefly, 100 µL of citrated PNP was added to the wells containing the surfaces that were previously exposed to plasma and t-PA. Following 5 min equilibration at 37 °C, 100 µL of 0.025×10^{-3} M $CaCl_2$ solution was added to the wells to initiate clotting. Absorbance at 405 nm was measured at 30 s intervals for 1h, using a microplate reader (Thermo Fisher Scientific, Inc.).

Cell Culture: HUVECs (Human umbilical vein endothelial cells) were seeded onto sample surfaces, which were placed in the wells of 48-well tissue culture plates, at a cell density of 12 000 cells per cm^2. The cells were incubated in endothelial cell medium (ECM) at 37 °C with 5% CO_2 in a humidified chamber for 4 and 48 h. After incubation, each sample was washed twice with sterilized PBS and fixed with 4% paraformaldehyde at room temperature for 10 min. Subsequently, the fixed cells were treated with 0.1% Triton X-100 for 5 min and then incubated with Actin-Tracker Green (Phalloidin-FITC, Sigma) in the dark for 40 min. After rinsing three times with sterilized PBS, the specimens were further stained with 4′,6-diamidino-2-phenylindole (DAPI, Sigma) for 10 min in the dark and then observed under an Olympus IX71 fluorescence microscope (Carl Zeiss, Germany) after thorougly washing with PBS. Each experiment was repeated three times and ten random images were acquired. The number of cells in each image was measured with the Image-Pro Plus software and the results were then averaged. The average number of cells was converted to the cell adhesion density.

Statistical Analysis: Each experiment was performed independently in duplicate at least, and quantified with at least triplicates. The results are expressed as the mean ± standard error of each sample. Statistical analysis was performed using OriginPro 8.0 software. One-way analysis of variance (ANOVA, *t*-test) was used to compare the data that were obtained with different samples under identical treatments. A difference with a p value of less than 0.05 was considered statistically significant.

Supporting Information

Supporting Information is available from the Wiley Online Library or from the author.

Acknowledgements

W.Z. and X.S. contributed equally to this work. This work was supported by the National Natural Science Foundation of China (21334004 and 21404076), the National Science Fund for Distinguished Young Scholars (21125418), the Natural Science Foundation of Jiangsu Province (BK20140316), and the Natural Sciences and Engineering Research Council of Canada. The authors appreciated Mr. Hao Gu and Miss Ting Wei for the help on in vitro hemocompatibility tests.

Received: April 23, 2015
Revised: June 21, 2015
Published online: July 14, 2015

[1] a) M. B. Gorbet, M. V. Sefton, *Biomaterials* **2004**, *25*, 5681; b) B. Furie, B. C. Furie, *New Engl. J. Med.* **2008**, *359*, 938; c) E. A. Vogler, C. A. Siedlecki, *Biomaterials* **2009**, *30*, 1857; d) S. Li, J. J. D. Henry, *Annu. Rev. Biomed. Eng.* **2011**, *13*, 451.

[2] a) N. Nakabayashi, D. F. Williams, *Biomaterials* **2003**, *24*, 2431; b) A. G. Kidane, H. Salacinski, A. Tiwari, K. R. Bruckdorfer, A. M. Seifalian, *Biomacromolecules* **2004**, *5*, 798; c) C. Werner, M. F. Maitz, C. Sperling, *J. Mater. Chem.* **2007**, *17*, 3376; d) X. Liu, L. Yuan, D. Li, Z. Tang, Y. Wang, G. Chen, H. Chen, J. L. Brash, *J. Mater. Chem. B* **2014**, *2*, 5718.

[3] H. Chen, L. Yuan, W. Song, Z. Wu, D. Li, *Prog. Polym. Sci.* **2008**, *33*, 1059.

[4] a) L. D. Unsworth, H. Sheardown, J. L. Brash, *Biomaterials* **2005**, *26*, 5927; b) Y. Chang, W. Chen, W. Yandi, Y. Shih, W. Chu, Y. Liu, C. Chu, R. Ruaan, A. Higuchi, *Biomacromolecules* **2009**, *10*, 2092; c) W. Guo, J. Zhu, Z. Cheng, Z. Zhang, X. Zhu, *ACS Appl. Mater. Interfaces* **2011**, *3*, 1675.

[5] a) H. Chen, Y. Chen, H. Sheardown, M. A. Brook, *Biomaterials* **2005**, *26*, 7418; b) D. Y. Lee, Z. Khatun, J. Lee, Y. Lee, I. In, *Biomacromolecules* **2011**, *12*, 336; c) M. Li, K. Neoh, E. Kang, T. Lau, E. Chiong, *Adv. Funct. Mater.* **2014**, *24*, 1631.

[6] a) D. Li, H. Chen, J. L. Brash, *Colloids Surf., B* **2011**, *86*, 1; b) J. C. Chapin, K. A. Hajjar, *Blood Rev.* **2015**, *29*, 17.

[7] a) W. G. McClung, D. L. Clapper, S. P. Hu, J. L. Brash, *Biomaterials* **2001**, *22*, 1919; b) H. Chen, Y. Zhang, D. Li, X. Hu, L. Wang, W. G. McClung, J. L. Brash, *J. Biomed. Mater. Res.* **2009**, *90A*, 940; c) D. Li, H. Chen, S. Wang, Z. Wu, J. L. Brash, *Acta Biomater.* **2011**, *7*, 954; d) Z. Wu, H. Chen, X. Liu, J. L. Brash, *Macromol. Biosci.* **2012**, *12*, 126; e) Z. Tang, D. Li, X. Liu, Z. Wu, W. Liu, J. L. Brash, H. Chen, *Polym. Chem.* **2013**, *4*, 1583.

[8] D. B. Cines, E. S. Pollak, C. A. Buck, J. Loscalzo, G. A. Zimmerman, R. P. McEver, J. S. Pober, T. M. Wick, B. A. Konkle, B. S. Schwartz, E. S. Barnathan, K. R. McCrae, B. A. Hug, A. M. Schmidt, D. M. Stern, *Blood* **1998**, *91*, 3527.

[9] a) L. P. Brewster, D. Bufallino, A. Ucuzian, H. P. Greisler, *Biomaterials* **2007**, *28*, 5028; b) A. P. McGuigan, M. V. Sefton, *Biomaterials* **2007**, *28*, 2547; c) Z. Yang, K. Xiong, P. Qi, Y. Yang, Q. Tu, J. Wang, N. Huang, *ACS Appl. Mater. Interfaces* **2014**, *6*, 2647.

[10] a) S. Lu, P. Zhang, X. Sun, F. Gong, S. Yang, L. Shen, Z. Huang, C. Wang, *ACS Appl. Mater. Interfaces* **2013**, *5*, 7360; b) Z. Yang, Y. Yang, W. Yan, Q. Tu, J. Wang, N. Huang, *ACS Appl. Mater. Interfaces* **2013**, *5*, 10495.

[11] a) A. P. Mould, A. Komoriya, K. M. Yamada, M. J. Humphries, *J. Biol. Chem.* **1991**, *266*, 3579; b) S. P. Massia, J. A. Hubbell, *J. Biol. Chem.* **1992**, *267*, 14019; c) H. Ceylan, A. B. Tekinay, M. O. Guler, *Biomaterials* **2011**, *32*, 8797; d) Y. Ji, Y. Wei, X. Liu, J. Wang, K. Ren, J. Ji, *J. Biomed. Mater. Res. A* **2012**, *100A*, 1287; e) Y. Wei, Y. Ji, L. L. Xiao, Q. K. Lin, J. P. Xu, K. F. Ren, J. Ji, *Biomaterials* **2013**, *34*, 2588.

[12] C. Nojiri, Y. Noishiki, H. Koyanagi, *J. Thorac. Cardiov. Sur.* **1987**, *93*, 867.

[13] a) F. Rusmini, Z. Zhong, J. Feijen, *Biomacromolecules* **2007**, *8*, 1775; b) P. Jonkheijm, D. Weinrich, H. Schroder, C. M. Niemeyer, H. Waldmann, *Angew. Chem. Int. Ed.* **2008**, *47*, 9618; c) Q. Yu, Y. Zhang, H. Wang, J. L. Brash, H. Chen, *Acta Biomater.* **2011**, *7*, 1550.

[14] a) Y. B. Lee, Y. M. Shin, J. Lee, I. Jun, J. K. Kang, J. Park, H. Shin, *Biomaterials* **2012**, *33*, 8343; b) P. H. Nilsson, K. N. Ekdahl, P. U. Magnusson, H. Qu, H. Iwata, D. Ricklin, J. Hong, J. D. Lambris, B. Nilsson, Y. Teramura, *Biomaterials* **2013**, *34*, 985.

[15] a) G. Cooke, V. M. Rotello, *Chem. Soc. Rev.* **2002**, *31*, 275; b) J. Zhang, P. X. Ma, *Nano Today* **2010**, *5*, 337; c) H. Yang, B. Yuan, X. Zhang, O. A. Scherman, *Acc. Chem. Res.* **2014**, *47*, 2106.

[16] a) G. Chen, M. Jiang, *Chem. Soc. Rev.* **2011**, *40*, 2254; b) O. Nachtigall, C. Kördel, L. H. Urner, R. Haag, *Angew. Chem. Int. Ed.* **2014**, *53*, 9669.

[17] a) A. Martinez, C. Ortiz Mellet, J. M. Garcia Fernandez, *Chem. Soc. Rev.* **2013**, *42*, 4746; b) X. Shi, G. Chen, L. Yuan, Z. Tang, W. Liu, Q. Zhang, D. M. Haddleton, H. Chen, *Mater. Horiz.* **2014**, *1*, 540.

[18] X. Shi, W. Zhan, G. Chen, Q. Yu, Q. Liu, H. Du, L. Cao, X. Liu, L. Yuan, H. Chen, *Langmuir* **2015**, *31*, 6172.

[19] Z. Wu, H. Chen, H. Huang, T. Zhao, X. Liu, D. Li, Q. Yu, *Macromol. Biosci.* **2009**, *9*, 1165.

[20] M. Husseman, E. E. Malmström, M. McNamara, M. Mate, D. Mecerreyes, D. G. Benoit, J. L. Hedrick, P. Mansky, E. Huang, T. P. Russell, C. J. Hawker, *Macromolecules* **1999**, *32*, 1424.

[21] X. H. Xiong, Z. Q. Wu, J. J. Pan, L. Xue, Y. J. Xu, H. Chen, *J. Mater. Chem. B* **2015**, *3*, 629.

[22] a) T. A. Horbett, *Colloids Surf., B* **1994**, *2*, 225; b) M. Mrksich, G. M. Whitesides, *Annu. Rev. Biophys. Biomol. Struct.* **1996**, *25*, 55; c) L. M. Szott, T. A. Horbett, *Curr. Opin. Chem. Biol.* **2011**, *15*, 683.

[23] a) K. Ishihara, K. Fukumoto, Y. Iwasaki, N. Nakabayashi, *Biomaterials* **1999**, *20*, 1553; b) M. C. Shen, M. S. Wagner, D. G. Castner, B. D. Ratner, T. A. Horbett, *Langmuir* **2003**, *19*, 1692; c) D. Kwak, Y. G. Wu, T. A. Horbett, *J. Biomed. Mater. Res.* **2005**, *74A*, 69; d) B. Sivaraman, R. A. Latour, *Biomaterials* **2010**, *31*, 832.

[24] K. A. Woodhouse, J. I. Weitz, J. L. Brash, *Biomaterials* **1996**, *17*, 75.

[25] X. Shi, G. Chen, Y. Wang, L. Yuan, Q. Zhang, D. M. Haddleton, H. Chen, *Langmuir* **2013**, *29*, 14188.

[26] P. Antoni, Y. Hed, A. Nordberg, D. Nyström, H. von Holst, A. Hult, M. Malkoch, *Angew. Chem. Int. Ed.* **2009**, *121*, 2160.